

Ca_{0.95}Nb₃O₆: Crystal and Electronic Structure

PERE ALEMANY,* VLADIMIR G. ZUBKOV,†
 SANTIAGO ALVAREZ,* VLADLEN P. ZHUKOV,†
 VALENTIN A. PERELIAEV,† IRINA KONTSEVAYA,†
 AND ALEXANDR TYUTYUNNIK†

**Departament de Química Inorgànica, Universitat de Barcelona, Diagonal 647, 08028 Barcelona, Spain, and † Institute of Solid State Chemistry, Pervomayskaya 91, 620219 Ekaterinburg, Russia*

Received April 20, 1992; in revised form November 2, 1992; accepted November 4, 1992

The title compound has been synthesized and its structure refined by using powder diffraction data. The structure is orthorhombic, space group *Immm*, with cell constants $a = 7.1156$ (9), $b = 10.2863$ (18), $c = 6.5756$ (9) Å, and $Z = 4$. Two types of Nb atoms are present in the structure: Nb1 atoms in Nb₂O₈ clusters with one of the shortest Nb–Nb distances known so far (2.560 Å), and Nb2 atoms forming layers of connected NbO₆ octahedra. The electronic structure obtained from Extended Hückel tight-binding band calculations suggests the coexistence of Nb(1+) ions in the Nb₂O₈ clusters with quadruple Nb–Nb bonds, together with Nb(4.5+) ions in the layers of octahedra. Deviations from this simplified model are analyzed. The electrical behavior, measured in the temperature range 4.2 K < T < 300 K, is metallic at low temperatures and practically temperature-independent at room temperature. A semimetallic character is proposed based on the calculated band electronic structure, with the states around the Fermi level localized mainly on the layers of octahedra parallel to the *ac* plane. © 1993 Academic Press, Inc.

In recent years two analogous Nb compounds, NaNb₃O₅F and Ca_{0.75}Nb₃O₆, have been synthesized and their crystal structures determined (1, 2). In the latter structure the positions of the calcium ions are partially occupied, and the stoichiometric compound CaNb₃O₆ was not obtained. Two types of Nb atoms with different coordination spheres are present in the crystal structure: the Nb1 atoms form Nb₂O₈ square prisms with one of the shortest known Nb–Nb bond distances (2.578 Å in Ca_{0.75}Nb₃O₆), while the Nb2 atoms form layers of connected octahedra with relatively long Nb–Nb distances. Despite the noninteger formal oxidation state of +3.5 for the Nb atoms, which might give rise to a metallic character, no electrical measurements have been reported for the above compounds. For all these reasons we attempted the syn-

thesis of the stoichiometric compound CaNb₃O₆, its crystal structure determination, and the study of its electrical resistivity and electronic structure.

Experimental

Synthesis of Ca_{0.95}Nb₃O₆

A mixture of CaO and Nb₂O₅ was reduced with acetylene soot by heating in vacuum at 1200–1250°C for 10 hr. The single-phase nature of the final product of sintering was confirmed by X-ray analysis using CuK α radiation. The compound is orthorhombic, space group *Immm*, with unit cell parameters $a = 7.1156$ (9), $b = 10.2863$ (18), $c = 6.5756$ (9) Å, and $Z = 4$. Spectrophotometric analyses yielded results fairly close to those

TABLE I
 ATOMIC COORDINATES (STANDARD DEVIATIONS IN PARENTHESES), THERMAL PARAMETERS (B_{iso}), AND SITE POPULATIONS (N_i) FOR $Ca_{0.95}Nb_3O_6$

Atom	Position	x/a	y/b	z/c	B_{iso}	N_i
Ca	4i	0.5	0.5	0.241 (1)	0.8 (1)	3.76 (6)
Nb1	4j	0.0	0.5	0.3053 (6)	0.1 (1)	4
Nb2	8n	0.2275 (5)	0.2783 (3)	0.5	0.2 (1)	8
O1	4g	0.5	0.6589 (5)	0.0	0.5 (1)	4
O2	4h	0.5	0.6624 (6)	0.0	0.5 (1)	4
O3	16o	0.8034 (3)	0.3667 (3)	0.2266 (3)	0.26 (3)	16

obtained from neutron powder diffraction studies.

Crystal Structure Determination

Neutron diffraction measurements were carried out with $\lambda = 1.5118 \text{ \AA}$ with double monochromatization by pyrographite and germanium. The neutron diffraction patterns were obtained in the range $10^\circ < 2\theta < 115^\circ$ at increments of 0.1° . A full-profile analysis of the diffraction data was performed using a computer code (3) of the Rietveld algorithm. The diffraction patterns were fitted to Gauss functions with the angular dependence

$$H_{1/2}^2 = U \tan^2\theta + V \tan^2\theta + W,$$

where $U = 0.8587$, $V = -1.2667$, and $W = 0.7951$. The number of reflections employed in the refinement was 222. The initial coordinates used were those obtained by Hibble *et al.* (1) for $Ca_{0.75}Nb_3O_6$. The convergence criteria $R_I = 5.8\%$, $R_{WP} = 6.0\%$, $R_{exp} = 5.5\%$ were achieved by assuming a partial occupation of the Ca (4i) sites, corresponding to the formula $Ca_{0.95}Nb_3O_6$. The resulting atomic positions are given in Table I. Electrical resistivity measurements were performed by a four-probe technique on a sintered polycrystalline sample of dimensions $10 \times 1 \times 1 \text{ mm}$, in the temperature range $4.2 \text{ K} < T < 300 \text{ K}$ (Fig. 1).

Discussion of the Structure

The structural data (Table I) are similar to those for the analogous compound

$Ca_{0.75}Nb_3O_6$. The small differences in bond lengths (Table II) are within the 3 standard deviations range. The building blocks of the three-dimensional network are NbO_6 octahedra of Nb2 atoms and dinuclear Nb_2O_8 square prisms of Nb1 atoms with a short Nb-Nb distance of $2.560 (6) \text{ \AA}$. The octahedra are connected by sharing vertices along the a direction and edges along the c direction, thus forming layers parallel to the ac plane, as seen in the projections of the structure shown in Fig. 2. The prisms have the Nb-Nb bonds along the c direction, and are only connected through the octahedra in all directions. A perspective drawing of one Nb_2O_8 prism together with the neighboring, edge-sharing Nb2 atoms is shown in Fig. 3.

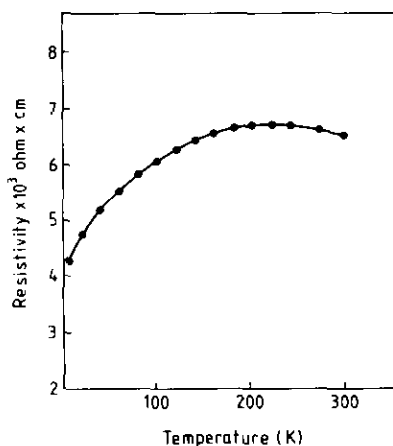


FIG. 1. Temperature dependence of the electrical resistivity of $Ca_{0.95}Nb_3O_6$.

TABLE II
 Nb–Nb BOND DISTANCES (Å) AND NbNbO BOND ANGLES (°) FOR THE $\text{A}_x\text{Nb}_3\text{X}_6$ COMPOUNDS

Atoms	Crystallographic direction	$\text{Ca}_{0.95}\text{Nb}_3\text{O}_6$	$\text{Ca}_{0.75}\text{Nb}_3\text{O}_6$	$\text{NaNb}_3\text{O}_5\text{F}$
Nb1–Nb1	<i>c</i>	2.560 (6)	2.578 (7)	2.614 (1)
Nb2–Nb2	<i>c</i>	3.348 (5)	3.357 (6)	
Nb2–Nb2	<i>a</i>	3.236 (5)	3.241 (6)	
Nb1–Nb2	<i>a + b</i>	3.073 (5)	3.061 (4)	3.09
Nb1–Nb1–O		104.8	104.0	103.7

Notice the similarity with the carboxylato-bridged complexes having metal–metal quadruple or triple bonds (4). One could alternatively describe such an arrangement of Nb atoms as an Nb_6 octahedral cluster, a common building block in Nb compounds (5), but it is a poor description of the geometry, given the large difference between the Nb1–Nb1 and Nb2–Nb2 distances (Table II).

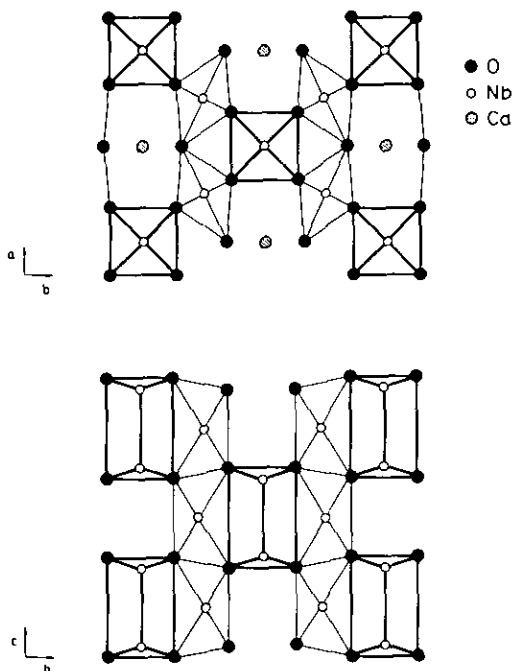


FIG. 2. Two projections of the structure of $\text{Ca}_{0.95}\text{Nb}_3\text{O}_6$. The thick lines correspond to the Nb_2O_8 square prisms of the Nb1 atoms, and the thin lines to the NbO_6 octahedra of Nb2 atoms.

Although several dinuclear Nb compounds exist (6), they are in most cases supported by bridging ligands, and a clear-cut bond order–bond distance correlation is not well established. The typical Nb–Nb bond distances for different oxidation states are summarized in Table III. Note, however, that the definition of metal–metal bond order is inaccurate when monoatomic bridges are present. An illustrative example (17) is given by $[\text{Nb}_2(\mu\text{-O})_3(\text{Ph}_4\text{porph})_2]$, where Ph_4porph is 5,10,15,20-tetraphenyl-prophyrinato. This is formally a compound of Nb(V) with a d^0 configuration and is expected to have no metal–metal bond, yet it presents Nb–Nb distances of 2.748 and 2.873 Å in two different solvates. An analy-

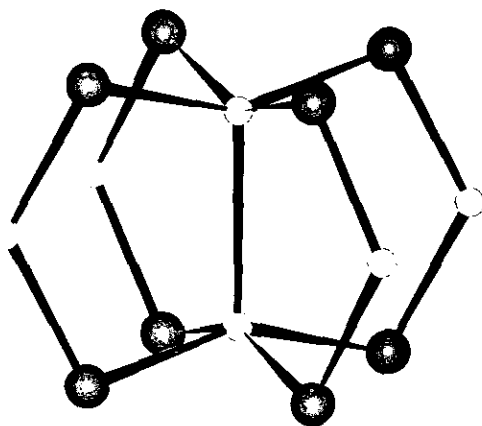


FIG. 3. Perspective drawing of the Nb_2O_8 cluster, showing the relative position of the neighboring Nb2 atoms.

TABLE III
BOND DISTANCES AND BOND ORDERS FOR Nb-Nb BONDS

Oxidation state	Geometry	Nb-Nb (Å)	Bond order	Refs.
I		≤ 2.6	4	^a
II	face-sharing octahedra unsupported <i>M-M</i>	2.60-2.63 ~ 2.70	3 3	(15)
III	edge-sharing octahedra ^b face-sharing octahedra	2.68-2.77 ≥ 2.73	2 2	(10-12, 14) (9, 10)
IV	edge-sharing octahedra	2.75-3.0 3.1-3.6	1 contacts	(7, 8) (16)
V	edge-sharing octahedra	> 3.7	0	(8)

^a Estimated, no experimental data available.

^b A few shorter (7*k*, 13) or longer (13*c*) bond distances can also be found.

sis of the effect of such bridges on Tc-Tc bonding has been presented elsewhere (18). According to our structural data (Table II) and the empirical criteria in Table III, the Nb1-Nb1 bonds in $\text{Ca}_{0.95}\text{Nb}_3\text{O}_6$ might be described as quadruple bonds, the Nb1-Nb2 as either a single bond or a contact, and the Nb2-Nb2 distances as nonbonding.

Electronic Band Structure

Tight-binding band calculations were performed for the anionic lattice $\text{Nb}_3\text{O}_6^{2-}$, within the extended Hückel formalism (see the Appendix for details), and adopting the experimental atomic positions of $\text{Ca}_{0.95}\text{Nb}_3\text{O}_6$. A detailed construction of the band structure of a Nb_3O_6 sublattice has previously been reported by Calhorda and Hoffmann (19) and we consequently omit the details, but discuss the bonding and formal oxidation states from a somewhat different viewpoint. A general description of the electronic structure can be obtained from the density of states (DOS) spectrum and its main contributions, shown in Fig. 4. The composition and bonding characteristics of the Nb1 and Nb2 bands were analyzed with the help of the COOP curves (COOP stands for *Crystal Orbital Overlap Population* (20)) between several atom pairs and between the σ -, π -, and δ -type orbitals of the Nb1 atoms, and the peaks in the DOS are accordingly la-

beled. At the lowest energies (below -14 eV) are the oxygen 2*s* and 2*p* levels. The set of bands between -11.5 and -14 eV and the one between -8.5 and -9.5 eV are mostly localized on the Nb1 atoms with metal-metal σ , π , and δ character, as indicated in Fig. 4, and mixing in some contributions from the Nb2 *d* orbitals. On the other hand, the bands between -9.5 and -11.5 as well as those above -8 eV arise primarily from the *d* orbitals of the Nb2 atoms, the lowest ones corresponding basically to the t_{2g} -like set expected for an approximately octahedral ligand field. The Fermi level (ϵ_F) for $\text{Nb}_3\text{O}_6^{2-}$ (with 53 valence electrons per formula unit) appears at -11.11 eV, resulting in a partial occupation of the lowest portion of the t_{2g} (Nb2) band. In contrast, for the Nb_3O_6^- sublattice (52 valence electrons), the t_{2g} band is the lowest empty one.

The outcome of such a band structure is that most of the 4*d* electron density is concentrated at the Nb1 atoms, therefore suggesting a mixed-valence compound. Since there are four electrons per repeat unit in the Nb1 bands, its formal oxidation state is +1, leaving nine positive charges (one electron) for two Nb2 atoms, i.e., a formal oxidation state of Nb2 of 4.5+.

The different localization of the bands outlined above and the resulting charge distribution between both types of Nb atoms can be associated with the *d* orbitals of the

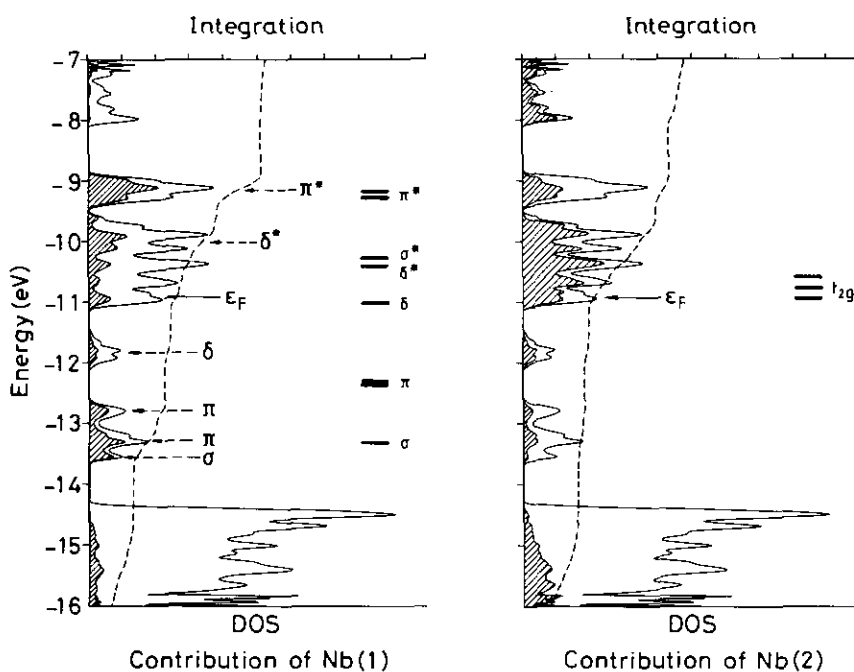


FIG. 4. Density of states (DOS) for the anionic $(\text{Nb}_3\text{O}_6)^{2-}$ sublattice of $\text{Ca}_{0.95}\text{Nb}_3\text{O}_6$. The shaded areas indicate the contribution of the Nb1 and Nb2 atoms to the total DOS, and the integrals of such contributions are represented by the dashed lines (full scale corresponds to 100%). The bars at the right-hand side of each diagram represent the energy of the d -block orbitals obtained from molecular orbital calculations on discrete clusters Nb_2O_8 (Nb1) and NbO_6 (Nb2).

discrete model clusters isolated from the crystal structure: Nb_2O_8 square prisms and NbO_6 octahedra. For Nb_2O_8 the expected levels are the σ , π , and δ bonding MOs and their antibonding counterparts δ^* , σ^* , and π^* , with the $d_{x^2-y^2}$ orbitals (Nb–O antibonding) at much higher energies. For the NbO_6 cluster, formally nonbonding t_{2g} and Nb–O antibonding e_g sets of orbitals appear. There is a neat correspondence between the molecular orbitals ordering in the clusters (shown in Fig. 4) and the band ordering in the solid, except that the π and δ bands appear at much lower energies than in the isolated cluster, a detail that will be discussed later on. A remarkable feature of the electronic structure of the $\text{Nb}_3\text{O}_6^{2-}$ sublattice is that the largest part of the Nb1–Nb1 bonding levels, below the Fermi level, are occupied, whereas the antibonding ones are empty. The result is an approximate elec-

tronic configuration $\sigma^2\pi^4\delta^2$ for the Nb1–Nb1 pairs with a calculated Nb1–Nb1 overlap population of 0.734. Note that the isostructural compounds $\text{NaNb}_3\text{O}_5\text{F}$, $\text{Ca}_{0.95}\text{Nb}_3\text{O}_6$, $\text{Ca}_{0.75}\text{Nb}_3\text{O}_6$, and the hypothetical NaNb_3O_6 differ in the occupation of the t_{2g} (Nb2) band of the anionic sublattice (1.0, 0.8, 0.5 and 0 electrons per formula unit containing two Nb2 atoms, respectively) and no differences in the Nb1–Nb1 bond strengths should be expected. Interestingly, small but significant variations in Nb1–Nb1 bond distance can be seen along the series (Table II), which can be associated with the differences in their Nb1–Nb1–O bond angles, as found for many multiply bonded M_2X_8 dinuclear compounds (21), rather than with their electron counts.

The highest occupied $4d$ levels are t_{2g} bands typical of octahedrally coordinated

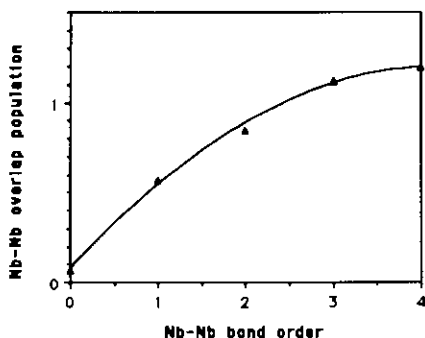
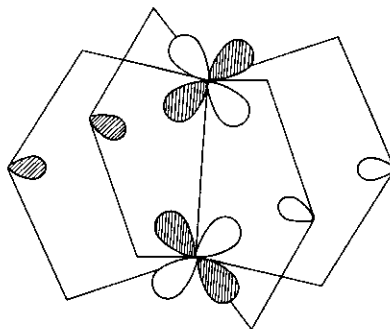


FIG. 5. Nb–Nb overlap population as a function of the formal bond order, calculated for $[\text{Nb}_2\text{O}_8]^{x-}$ clusters. See the Appendix for computational details.

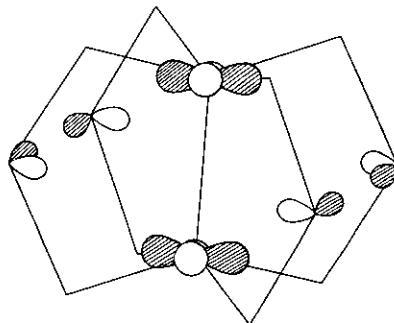
metal atoms; hence the electronic configuration for the Nb2 atoms in the $\text{Nb}_3\text{O}_6^{2-}$ sublattice is roughly $t_{2g}^{0.5}$. The calculated Nb2–Nb2 overlap population is 0.004, consistent with the Nb2–Nb2 nonbonding character found for the t_{2g} band and in good agreement with the long experimental Nb2–Nb2 distance of 3.348 Å. The unusually short Nb–Nb distance found for the Nb1 atoms in $\text{Ca}_{0.95}\text{Nb}_3\text{O}_6$ and its isostructural analogues (1, 2) $\text{Ca}_{0.75}\text{Nb}_3\text{O}_6$ and $\text{NaNb}_3\text{O}_5\text{F}$ is compatible with its formal description as a quadruple bond (Table III). Although the Nb1–Nb1 distances in the Nb_3X_6^n lattices are the shortest ones known so far, the lack of structural data for well established, unsupported Nb–Nb quadruple bonds makes the use of the bond length criterion inconclusive for deciding on the existence of a quadruple bond in this series of compounds. One can attempt to calibrate the Nb–Nb overlap populations obtained from band calculations by performing molecular orbital calculations on model dinuclear compounds $\text{Nb}_2\text{O}_8^{x-}$ with unambiguous bond orders. The resulting calibration curve is presented in Fig. 5, where the bond order coincides with the number of d electrons per Nb atom. Surprisingly, the Nb1–Nb1 overlap population obtained from band calculations on $\text{Nb}_3\text{O}_6^{2-}$ (0.73) is sensibly smaller than expected for a quadruple or even a triple bond. If a band calculation

is performed on a sublattice without the Nb2 atoms, $(\text{NbO}_6)^{11-}$, with the unambiguous oxidation state of Nb1(1+), the calculated Nb1–Nb1 overlap population is 1.18, consistent with the value found in our calibration curve (Fig. 5) for a discrete cluster with a quadruple bond. The small Nb1–Nb1 overlap population in $(\text{NbO}_6)^{11-}$ is therefore related to the existence of the Nb2 atoms in the lattice at relatively short distance (3.073 Å).

It is found that the t_{2g} orbitals of a Nb2 atom act as acceptors of electron density



SCHEME 1



SCHEME 2

from the π (Scheme 1) and δ (Scheme 2) occupied levels. This can be detected in our calculations (a) in the displacement of the π and δ bands to lower energies (Fig. 4) relative to the corresponding molecular orbitals of the Nb_2O_8 cluster, (b) in the incorporation of some Nb1–Nb2 bonding character into these bands, and (c) in the broadening of the empty t_{2g} band of Nb2

relative to an isolated NbO_6 octahedron, and its incorporation of Nb1–Nb2 antibonding character. Inclusion of the Nb2 atoms in the octahedral holes of the $(\text{NbO}_6)^{11-}$ sublattice results in the net transfer of 2.28 electrons from the π ($1.10 e^-$) and δ ($1.18 e^-$) orbitals of each Nb1 atom to the t_{2g} orbitals of the Nb2 atoms, resulting in $\text{Nb1}^{+1.72}$ for which the Nb1–Nb1 overlap population is expected to be 0.81 (Fig. 5), in good agreement with the value found in the band calculations for the solid. The calculated Nb1–Nb2 overlap population of 0.168, on the other hand, is consistent with a weak bond or *contact* (Fig. 5), as expected on an empirical basis (Table II) for the experimental bond length (3.073 Å).

According to the description of the electronic structure in the preceding section, the electrical conductivity must be associated with the octahedral Nb2 atoms. In contrast with the prediction of semiconducting properties for the hypothetical NaNb_3O_6 phase (19), a semimetallic character for all three existing compounds, $\text{Ca}_{0.95}\text{Nb}_3\text{O}_6$, $\text{Ca}_{0.75}\text{Nb}_3\text{O}_6$, and $\text{NaNb}_3\text{O}_5\text{F}$, stems from the present study.

Concluding Remarks

The compound with the composition $\text{Ca}_{0.95}\text{Nb}_3\text{O}_6$ has been prepared and its structure solved by means of a Rietveld analysis of its neutron diffraction patterns. Its electrical conductivity, measured down to 4.2 K, shows a peculiar temperature dependence.

The analogies between the band structure of the anionic sublattice $\text{Nb}_2\text{O}_8^{2-}$ and the molecular orbitals of Nb_2O_8 square prismatic and NbO_6 octahedral groups have been stressed. These analogies are useful for a simple description of the main peaks in the density of states plot and for the interpretation of their bonding properties. In a first approximation, the metal–metal bonding in this compound can be described as Nb1–Nb1 quadruple bonds bridged by four Nb2 atoms. Electron donation from the

Nb1–Nb1 pairs to the Nb2 atoms effectively decrease the Nb1–Nb1 bond order. Hence the possibility exists that replacement of Nb2 by metals with an increasing number of electrons in the t_{2g} subshell and decreasing acceptor abilities, could give rise to still shorter Nb1–Nb1 bonds. Both theoretical and empirical criteria for the assignment of formal bond orders to Nb–Nb interatomic distances have been established. Small variations in the Nb1–Nb1 bond distances in a series of isostructural compounds have been shown to be related to variations in the pyramidal angles around the Nb1 atoms rather than to differences in the electron counts, as found for dinuclear coordination compounds with metal–metal multiple bonds.

According to our theoretical analysis, the phases corresponding to the formula $\text{Ca}_x\text{Nb}_3\text{O}_6$ ($0.5 < x \leq 1$) are semimetallic, and the conductivity is associated with the octahedrally coordinated Nb2 atoms. In contrast, the hypothetical compound with one less electron in the anionic sublattice, NaNb_3O_6 , must be a semiconductor, and compounds ANb_3O_6 ($A = \text{trivalent cation}$) must be metallic.

Appendix: Computational Details

The qualitative theoretical discussions in this paper are based on molecular orbital (22) and tight-binding band calculations (23, 24) of the extended Hückel type with modified Wolfsberg–Helmholz formula (25), using the atomic parameters shown in Table IV. Molecular Orbital calculations were carried out on the model compounds $[\text{Nb}_2\text{O}_8]^{n-}$ ($n = 6 - 14$) and $[\text{NbO}_6]^{7-}$ using the experimental bond distances and angles for Nb1 and Nb2, respectively. Average properties were calculated using a set of 48 k -points chosen according to the geometrical method of Ramírez and Böhm (27). Since the formal oxidation state of +4.5 found for the Nb2 atoms would be consistent with higher ionization potentials than for Nb1, several control calculations were carried out increasing the H_{ii} 's of Nb2 by up to 2 eV, and our

TABLE IV
ATOMIC PARAMETERS FOR EXTENDED HÜCKEL CALCULATIONS

Atom	Orbital	H_{ii}	ζ_{i1} (c_1)	ζ_{i2} (c_2)	Ref.
Nb	5s	-10.10	1.89		(26)
	5p	-6.86	1.85		
	4d	-12.10	4.08 (0.6401)	1.64 (0.5516)	
O	2s	-32.3	2.275		(22)
	2p	-14.8	2.275		

Note. H_{ii} 's are the orbital ionization energies, ζ_{ij} the Slater exponents, and c_j the coefficients in the double- ζ expansion of the d orbitals.

qualitative conclusions remained unchanged.

Acknowledgments

Financial support for the research at Barcelona was given by CICYT through Grant PB89-0268. The authors are grateful to the Institut d'Estudis Catalans for making the stay of V. P. Zhukov at Barcelona possible and to F. Vilardell for the drawings. P. Alemany thanks the Ministerio de Educaió y Ciencia for a fellowship of the Plan Nacional de Nuevos Materiales.

References

1. S. J. HIBBLE, A. K. CHEETHAM, AND D. E. COX, *Inorg. Chem.* **26**, 2389 (1987).
2. J. KÖHLER AND A. SIMON, *Angew. Chem. Int. Ed. Engl.* **25**, 996 (1986).
3. A. W. HEWAT, *Nucl. Instrum. Meth.* **127**, 361 (1975).
4. F. A. COTTON AND R. A. WALTON, "Multiple Bonds Between Metal Atoms," 2nd. ed. Wiley, New York (1993); *Struct. Bonding* **62**, 1 (1985), and references within.
5. R. P. ZIEBARTH, AND J. D. CORBETT, *Acc. Chem. Res.* **22**, 256 (1989).
6. C. E. HOLLOWAY, AND M. MELNIK, *Rev. Inorg. Chem.* **7**, 161 (1985).
7. (a) M. G. B. DREW, D. A. RICE, AND D. M. WILLIAMS, *Acta Crystallogr. Sect. C* **40**, 1547 (1984); (b) M. G. B. DREW, D. A. RICE, AND D. M. WILLIAMS, *J. Chem. Soc. Dalton Trans.* 1087 (1984); (c) F. A. COTTON, S. A. DURAJ, AND W. J. ROTH, *Inorg. Chem.* **23**, 3592 (1984); (d) P. D. W. BOYD, A. J. NIELSON, AND C. E. F. RICKARD, *J. Chem. Soc. Dalton Trans.* 307 (1987); (e) A. J. BENTON, M. G. B. DREW, R. J. HOBSON, AND D. A. RICE, *J. Chem. Soc. Dalton Trans.* 1304 (1981); (f) M. G. B. DREW, D. A. RICE, AND D. M. WILLIAMS, *J. Chem. Soc. Dalton Trans.* 417 (1985); (g) F. A. COTTON, M. P. DIEBOLD, AND W. J. ROTH, *Inorg. Chem.* **26**, 3319 (1987); (h) J. A. M. CANICH, F. A. COTTON, L. R. FALVELLO, AND S. A. DURAJ, *Inorg. Chim. Acta* **143**, 185 (1988); (i) K. TATSUMI, Y. SEKIGUCHI, M. SEBATA, A. NAKAMURA, R. E. CRAMER, AND T. CHUNG, *Angew. Chem. Int. Ed. Engl.* **28**, 98 (1989); (j) S. J. BENTON, M. G. B. DREW, R. J. HOBSON, D. A. RICE, *J. Chem. Soc. Dalton Trans.* 1304 (1981); (k) F. A. COTTON, M. P. DIEBOLD, AND W. J. ROTH, *Inorg. Chem.* **24**, 3509 (1985); (l) G. C. CAMPBELL, J. A. M. CANICH, F. A. COTTON, S. A. DURAJ, J. F. HAW, *Inorg. Chem.* **25**, 287 (1986); and (m) M. G. B. DREW, I. B. BABA, D. A. RICE, AND D. M. WILLIAMS, *Inorg. Chim. Acta* **44**, 217 (1980).
8. (a) D. R. TAYLOR, J. C. CALABRESE, AND E. M. LARSEN, *Inorg. Chem.* **16**, 721 (1977); (b) A. K. CHEETHAM, AND C. N. R. RAO, *Acta Crystallogr. Sect. B Struct. Crystallogr. Cryst. Chem.* **32**, 1579 (1976).
9. (a) J. L. TEMPLETON, W. C. DORMAN, J. C. CLARDY, AND R. E. MCCARLEY, *Inorg. Chem.* **17**, 1263 (1978). (b) F. A. COTTON, S. A. DURAJ, L. R. FALVELLO, AND W. J. ROTH, *Inorg. Chem.* **24**, 4389 (1985).
10. J. A. M. CANICH, AND F. A. COTTON, *Inorg. Chem.* **26**, 4236 (1987).
11. E. BABAIAK-KIBALA, F. A. COTTON, AND P. A. KIBALA, *Inorg. Chem.* **29**, 4236 (1990).
12. F. A. COTTON AND M. SHANG, *Inorg. Chem.* **29**, 508 (1990).
13. (a) F. A. COTTON, M. P. DIEBOLD, AND W. J. ROTH, *Inorg. Chem.* **26**, 3323 (1987); (b) F. A. COTTON, M. P. DIEBOLD, AND W. J. ROTH, *Inorg. Chem.* **24**, 3509 (1985); and (c) G. MEYER, AND R. HOPPE, *Z. Anorg. Allg. Chem.* **424**, 128 (1976).
14. F. A. COTTON, AND W. J. ROTH, *Inorg. Chem.* **22**, 3654 (1983).
15. F. A. COTTON, M. P. DIEBOLD, W. J. ROTH, *J. Am. Chem. Soc.* **109**, 5506 (1987).
16. A. ZALKIN AND D. E. SANDS, *Acta Crystallogr.* **11**, 615 (1958).
17. (a) C. LECOMTE, J. PROTAS, R. GUILARD, B. FLINIAUX, AND P. FOURNARI, *J. Chem. Soc. Dalton*

- Trans.* 1306 (1979); (b) J. F. JOHNSON, AND W. R. SCHEIDT, *Inorg. Chem.* **17**, 1280 (1978).
18. A. W. E. CHAN, R. HOFFMANN, AND S. ALVAREZ, *Inorg. Chem.* **30**, 1086 (1991).
19. M. J. CALHORDA, AND R. HOFFMANN, *J. Am. Chem. Soc.* **110**, 8376 (1988).
20. (a) T. HUGHBANKS, AND R. HOFFMANN, *J. Am. Chem. Soc.* **105**, 3528 (1983); (b) R. HOFFMANN, "Solids and Surfaces. A Chemist's View of Bonding in Extended Structures," VCH, New York (1988).
21. J. LOSADA, S. ALVAREZ, J. J. NOVOA, F. MOTA, R. HOFFMANN, AND J. SILVESTRE, *J. Am. Chem. Soc.* **112**, 8998 (1990); F. MOTA, J. J. NOVOA, J. LOSADA, S. ALVAREZ, R. HOFFMANN, AND J. SILVESTRE, *J. Am. Chem. Soc.*, in press.
22. R. HOFFMANN, *J. Chem. Phys.* **39**, 1397 (1963); R. HOFFMANN, AND W. N. LIPSCOMB, *J. Chem. Phys.* **36**, 2179, 2872, and 3489 (1962).
23. M.-H. WHANGBO, AND R. HOFFMANN, *J. Am. Chem. Soc.* **100**, 6093 (1978).
24. M.-H. WHANGBO, R. HOFFMANN, AND R. B. WOODWARD, *Proc. R. Soc. London Ser. A* **366**, 23 (1979).
25. J. H. AMMETER, H.-B. BÜRGI, J. C. THIBEAULT, AND R. HOFFMANN, *J. Am. Chem. Soc.* **100**, 3686 (1978).
26. R. H. SUMMERVILLE AND R. HOFFMANN, *J. Am. Chem. Soc.* **98**, 7240 (1976).
27. R. RAMÍREZ, AND M. C. BÖHM, *Int. J. Quantum Chem.* **34**, 571 (1988); **30**, 391 (1986).